Li et al. Nanoscale Research Letters (2015) 10:144
DOI 10.1186/s11671-015-0850-2

Nanoscale Research Letters
a SpringerOpen Journal

NANO EXPRESS Open Access

A facile hydrothermal approach to the synthesis of nanoscale rare earth hydroxides

Chengyin Li[1,2], Hui Liu[1] and Jun Yang[1*]

Abstract

Nanosized rare earth (RE) hydroxides including $La(OH)_3$, $Nd(OH)_3$, $Pr(OH)_3$, $Sm(OH)_3$, $Gd(OH)_3$, and $Er(OH)_3$ with rod-like morphology are fabricated via a convenient hydrothermal approach. This strategy calls for the first preparation of metal complexes between RE precursors and dodecylamine (DDA) in water/ethanol mixture at room temperature and subsequent thermal decomposition at elevated temperature. The influence of reaction time and water/ethanol volume ratios on the morphology and size of as-prepared RE hydroxides are investigated. CeO_2 nanoparticles with spherical shape could be directly obtained by hydrothermal treatment of complexes formed between Ce precursors and DDA. In addition, by further calcinating the RE hydroxides at high temperature in air, RE oxide nanorods could be readily produced.

Keywords: Rare earth; Hydrothermal; Hydroxide; Nanorod; Oxide

Background

Recent years have witnessed considerable interest in the design and preparation of rare earth (RE) nanomaterials due to their great potential applications as phosphors, magnets, catalysts, superconductors, and electrolytes [1-8]. In general, the physical and chemical properties of nanomaterials are closely related to their size, chemical composition, and morphology, which render the synthesis of nanosized RE materials an important prerequisite for further scientific or industrial investigations [9]. Among a large number of nanosized RE candidates, the RE hydroxides, which can be easily modified into corresponding oxides, oxysulfides, oxyfluorides, and fluorides, have attracted much attention in recent years [10-14].

So far, the preparation of the nanosized RE hydroxides is mainly based on a hydrothermal/solvothermal treatment in the presence of an inorganic base/organic base at a designed temperature. Typically, a hydrothermal system for preparing RE hydroxides consists of precursor, solvent, and organic additive. The RE precursors are usually simple nitrates or chlorides. The solvent mainly includes water, ethanol, and ethylene glycol. As the physicochemical properties of the solvent can influence reactivity, solubility, and diffusion behavior of the reagents, different solvents benefit morphology and size control. For instance, ethanol, with low RE^{3+} solubility, and ethylene glycol, with high viscosity and tunable diffusion rate of ions, both have been proved to be effective solvents to slow down the nucleation and growth rate of nanoparticles [15]. Besides, a great number of reports have demonstrated that, in the hydrothermal method, the most efficient and straightforward strategy for fine-tuning the shape and size of a targeted material is to select addition of organic additives, including hydrophilic and hydrophobic ones. On the one hand, the coordination effect between the hydrophilic ligands and RE ions will affect the actual concentration of free ions, thereby influencing the concentration of monomer and growth kinetics. On the other hand, the selective adsorption of ligands on different facets of crystallites favors morphology control.

In this work, we demonstrate a hydrothermal approach to the fabrication of RE hydroxide nanorods, labeled as $RE(OH)_3$ (RE = La, Nd, Pr, Sm, Gd, and Er). This strategy is based on the thermal decomposition of metal complexes formed by RE precusors and dodecylamine at room temperature. As we will demonstrate, the RE hydroxide nanorods could be further manipulated into corresponding nanosized RE oxides via a simple calcination procedure. Considering the remarkable simplicity of the synthetic approaches, the studies in this work might be promising for

* Correspondence: jyang@ipe.ac.cn
[1]State Key Laboratory of Multiphase Complex Systems, Institute of Process Engineering, Chinese Academy of Sciences, Beijing 100190, China
Full list of author information is available at the end of the article

creating nanosized RE hydroxides and RE oxides on a large scale for a given technological application (e.g., as phosphors, magnets, and catalysts)

Methods

General materials

The RE precursors, including lanthanum(III) nitrate ($La(NO_3)_3{\cdot}6H_2O$, 99%), praseodymium(III) nitrate ($Pr(NO_3)_3{\cdot}6H_2O$, 99%), neodymium(III) nitrate ($Nd(NO_3)_3{\cdot}6H_2O$, 99%), samarium(III) nitrate ($Sm(NO_3)_3{\cdot}6H_2O$, 99%), gadolinium(III) nitrate ($Gd(NO_3)_3{\cdot}6H_2O$, 99%), and erbium(III) nitrate ($Er(NO_3)_3{\cdot}5H_2O$, 99.9%), were from Aladdin Reagents, Shanghai, China; cerium(III) nitrate ($Ce(NO_3)_3{\cdot}6H_2O$, 99%) was from Sinopharm Chemical Reagent Co., Ltd., Beijing, China; ethanol (99.5%) was from Beijing Chemical Works, Beijing, China; and dodecylamine (DDA, 98%) was from J&K Scientific Ltd., Beijing, China. All glassware and autoclave Teflon liner were cleaned with *aqua regia*, followed by copious rinsing with deionized water before drying in an oven.

Synthesis of lanthanide hydroxide nanoparticles

In a typical synthesis of RE hydroxide nanorods, 0.2 mmol of RE precursors ($La(NO_3)_3$, $Pr(NO_3)_3$, $Nd(NO_3)_3$, $Sm(NO_3)_3$, $Gd(NO_3)_3$, $Er(NO_3)_3$, or $Ce(NO_3)_3$) was dissolved in 10 mL of deionized water, and then 10 mL of ethanol containing 5 mL of DDA was added. After sufficient mixing, the mixture was transferred into an autoclave with a volume of 50 mL, which was kept at 180°C for 18 h. After the hydrothermal process, the autoclave was cooled down to room temperature naturally, and the precipitates were collected by centrifugation and washed with deionized water and pure ethanol for several times. Finally, the products were dried at 60°C for structural characterizations. Further, the RE oxides (La_2O_3, Pr_6O_{11}, Nd_2O_3, and Er_2O_3) were produced by calcinating their corresponding RE hydroxides at 600°C for 2 h in air.

Characterization

Fourier transform infrared spectroscopy (FTIR) analysis was performed on a Bruker Alpha RT-DLATGS spectrometer (Bruker Optik Gmbh, Ettlingen, Germany). The spectra were collected over the range of 400 to 4,000 cm^{-1} in the transmission mode. Powder X-ray diffraction (XRD) measurements were carried out on a Bruker D8 focus X-ray diffractometer (Bruker Optik Gmbh, Ettlingen, Germany), using Cu-Kα radiation ($\lambda = 1.5406$ Å). TEM and high-resolution TEM (HRTEM) were performed on the JEOL JEM-2100 (JEOL Ltd., Akishima, Tokyo, Japan) and FEI Tecnai G^2 F20 electron microscope (FEI, Hillsboro, OR, USA) operating at 200 kV with a supplied software for automated electron tomography. For the TEM measurements, a drop of the nanoparticle solution was dispensed onto a 3-mm carbon-coated copper grid. Excessive solution was removed by an absorbent paper, and the sample was dried at room temperature in air.

Results and discussion

It has been demonstrated that the DDA can interact with almost all transition and noble metal ions to form metal complexes soluble in non-polar organic solvents [16]. Similarly, upon mixing the aqueous solution of RE precursors and ethanolic solution of DDA, metal complexes composed of RE precursors and DDA could also be formed. Ethanol was used to ensure the sufficient contact between RE precursors and DDA since it is water-miscible and a good solvent for DDA. The formation of RE precursor-DDA complexes could be verified by the FTIR spectra of the compounds recovered from the mixture of aqueous RE precursor solution and ethanolic DDA solution. As shown in Additional file 1: Figure S1 for the FTIR spectra of pure DDA, the bands at 3,338, 2,918, and 1,473 cm^{-1} are attributed to the stretching vibrations of C-N, C-H, and N-H, respectively. In comparison with that of pure DDA, apparent differences could be identified in the N-H and C-N stretching vibrations while other FTIR characteristic peaks are remained in RE precursor-DDA compounds (Additional file 1: Figure S1), demonstrating that there was a strong coordination effect between the NH_2 group in DDA and RE precursors.

The RE precursor-DDA complexes are then decomposed at elevated temperature, resulting in the generation of RE hydroxide products, labeled as $RE(OH)_3$, which subsequently grow into $RE(OH)_3$ nanorods and are protected by DDA. The possible mechanism accounting for the formation of $RE(OH)_3$ might resemble the preparation of lanthanide hydroxide using oleylamine [13] or triethylamine [17] as organic additives, the protonation of which leads to the generation of hydroxyl ions from water solvent for the formation of hydroxides. In this work, DDA provides the basic environment for the formation of RE hydroxides. Figure 1 shows the XRD patterns of $RE(OH)_3$ samples. All the diffraction peaks can be readily indexed to the pure hexagonal phase. The peaks are steep and high, and no additional peaks of other phases have been found, indicating that the $RE(OH)_3$ products are well crystallized and of high purity. The lattice constants (a and c) were calculated and listed in Additional file 1: Table S1. The decrease in lattice constants from Pr to Er hydroxides can be attributed to the well-known lanthanide contraction [18,19].

The size and morphology of the RE hydroxide products were examined by TEM. As exhibited in Figure 2, most of these hydroxide products have rod-like structure with lengths up to a few hundreds of nanometers. The histograms resulting from counting 100 well-separated particles (Additional file 1: Figure S2) depict that the average diameters are of ca. 10 to 50 nm (12.2 nm for La

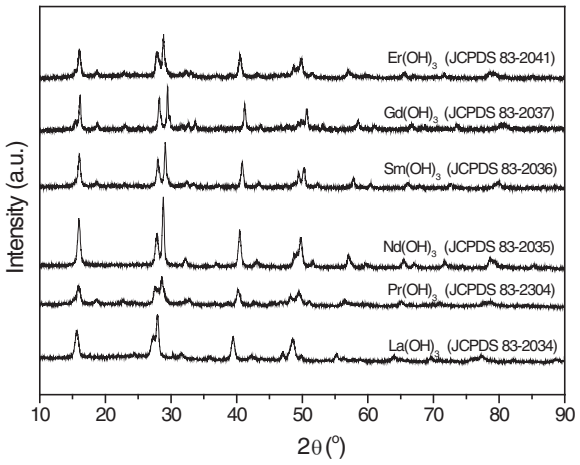

Figure 1 XRD patterns of RE hydroxides as prepared by decomposing the RE precursor-DDA complexes at elevated temperature.

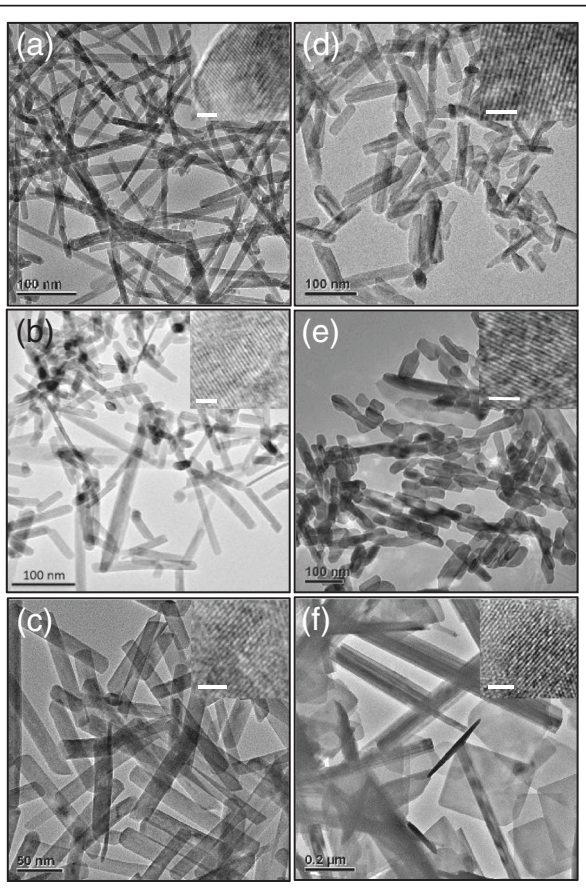

Figure 2 TEM and HRTEM images. $La(OH)_3$ **(a)**, $Pr(OH)_3$ **(b)**, $Nd(OH)_3$ **(c)**, $Sm(OH)_3$ **(d)**, $Gd(OH)_3$ **(e)**, and $Er(OH)_3$ **(f)** as synthesized by decomposing the RE precursor-DDA complexes at elevated temperature. The scale bar for the HRTEM images (inset of each TEM image) is 2 nm.

$(OH)_3$, 14.2 nm for $Pr(OH)_3$, 18.8 nm for $Nd(OH)_3$, 33.4 nm for $Sm(OH)_3$, 18.3 nm for $Gd(OH)_3$, and 44.2 nm for $Er(OH)_3$, respectively). In addition, for Er $(OH)_3$, a number of nanosheets are also observed in the TEM image (Figure 2f). The HRTEM images (insets of each TEM image) indicate that the RE hydroxide nanorods are highly crystallized. It has been believed that the driving force for the anisotropic growth of $RE(OH)_3$ nanorods derives from the inherent crystal structure of $RE(OH)_3$ materials. As indicated by the XRD patterns (Figure 1), the as-prepared RE hydroxides have hexagonal structures. Their $P6_3/m$ space group is usually favorable to the formation of hexagonal rods or plates [9]. However, the influence of the DDA on the anisotropic growth of $RE(OH)_3$ cannot be ruled out. The anisotropic adsorption of DDA on the surface of the growing $RE(OH)_3$ products and the structure of RE precursor-DDA complexes might have contribution to the formation of $RE(OH)_3$ nanorods, analogous to the worm-like Pd nanoparticles derived from coordinating compounds formed between $PdCl_2$ and DDA [16].

A special case was observed for the cerium system. Instead of $Ce(OH)_3$ nanorods, the hydrothermal treatment of complexes formed by $CeNO_3$ and DDA at 180°C results in the formation of CeO_2 nanoparticles with spherical shapes, as shown by the TEM and HRTEM images in Additional file 1: Figure S3. The nanoparticles are well defined and have an average diameter of ca. 13.2 nm. The XRD pattern (Additional file 1: Figure S3b) illustrates that the CeO_2 nanoparticles prepared this way have cubic structure (JCPDS card file: 780694). It should be emphasized that although we cannot rule out the $Ce(OH)_3$ which is an intermediate product during the hydrothermal treatment of $Ce(NO_3)_3$-DDA complexes, all attempts (e.g., altering temperature, DDA/$Ce(NO_3)_3$ ratios, reaction time, or water/ethanol volume ratios) to prepare $Ce(OH)_3$ products were unsuccessful. This may be interpreted that Ce $(OH)_3$ is quite unstable and easy to be decomposed at elevated temperature. The Ce(III) ions are then further oxidized to Ce(IV) by air, leading to the generation of CeO_2 nanoparticles protected by DDA. The stabilization by capping agent (DDA) is important to retain the crystal structure of CeO_2 as the cubic phase is not a common product under ambient conditions for light and medium RE oxides [9].

After hydrothermal treatment, the FTIR spectra of the products (Additional file 1: Figure S4) provides evidence for the presence of hydroxyl groups, as indicated by the strong bonds around 3600 cm^{-1} (except for Ce(III)-DDA system). In addition, after copious washing by water and ethanol, the DDA, which serves as capping agent for the hydroxide or oxide products, is still detectable in the FTIR spectra, as displayed by the stretching vibrations of N-H (ca. 1,500 cm^{-1}) and C-H (ca. 2,900 cm^{-1}).

Taking $La(OH)_3$ as a typical example, we have conducted a series of experiments under different hydrothermal

conditions to investigate the growth of RE hydroxide nanorods. We found that the reaction time and water/ethanol volume ratio have significant influence on the size and morphology of the RE hydroxides, while the effect from the hydrothermal temperature and DDA/RE precursor ratio is only slight. Figure 3a,b,c,d shows the TEM images of $La(OH)_3$ nanorods as prepared by hydrothermal treatment of $La(NO_3)_3$-DDA complexes at 180°C for 6, 12, 18, and 24 h, respectively. At 6 h, only short $La(OH)_3$ nanorods are observed under TEM (Figure 3a). At longer time (12 h), the length of the nanorods become larger while the diameter of the rods are remained (Figure 3b), indicating that the anisotropic growth of $La(OH)_3$ occurs along the axial direction. After 18 h, the $La(OH)_3$ nanorods are fully developed, and further increase in reaction time would not alter the morphology and size of the final $La(OH)_3$ nanorods (Figure 3c,d).

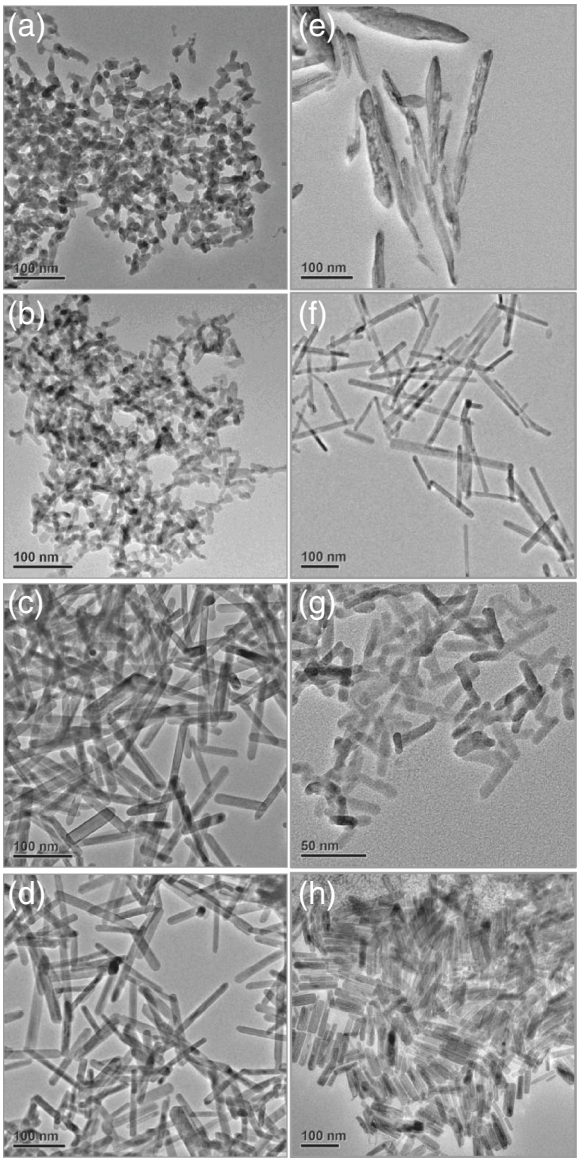

Figure 3 TEM images of $La(OH)_3$ nanorods. Prepared under different reaction times and water/ethanol volume ratios: **(a-d)** 6, 12, 18, and 24 h while DDA volume and water/ethanol volume ratio are fixed at 5 mL and 1/1, respectively; **(e-h)** water/ethanol volume ratio of 100/0, 80/20, 20/80, and 0/100 while DDA and reaction time are fixed at 5 mL and 18 h, respectively.

The TEM images of the $La(OH)_3$ nanorods as prepared by the hydrothermal approach under different water/ethanol volume ratios are shown in Figure 3e,f,g,h. As indicated, at water/ethanol volume ratios of 100:0 (Figure 3e), 80:20 (Figure 3f), 20:80 (Figure 3g), and 0:100 (Figure 3h), $La(OH)_3$ nanomaterials with rod-like morphology are formed as dominant products. However, as illustrated by these TEM images, the $La(OH)_3$ nanorods synthesized at water/ethanol ratio of 80:20 have a larger aspect ratio (Figure 3f), while those synthesized at water/ethanol ratio of 0:100 are more uniform in length and diameter (Figure 3h).

It is well known in colloidal chemistry method that nanoparticles are formed via two processes, i.e., nucleation and crystal growth [20,21]. The nucleation is usually determined by the supersaturation and temperature, while the particle growth is a process of the assembling of atoms on the surface of nuclei, which could be controlled by the diffusion of atom to the growing surface followed by the incorporation into the lattice. The incorporation process might be associated with the formation of chemical bond, which could be regarded as a reaction step. Both the diffusion step and the reaction step can affect the particle formation. The compromise of diffusion step and reaction step might be an important prerequisite to facilitate the formation of nanoparticles with uniform size and narrow size distribution [22]. The ratio of water/ethanol could affect the diffusion of $La(OH)_3$ reactants generated from the decomposition of $La(NO_3)_3$-DDA complexes by effectively regulating the viscosity of the mixture and hence results in the formation of $La(OH)_3$ nanorods with different sizes and morphologies.

By further calcinating the $RE(OH)_3$ hydroxides at 600°C for 2 h, corresponding RE oxides could be obtained easily [17,23,24]. La_2O_3, Pr_6O_{11}, Nd_2O_3, and Er_2O_3 have been prepared this way and confirmed by XRD patterns (Additional file 1: Figure S5), which manifest the as-obtained La_2O_3 and Nd_2O_3 oxides that remain the hexagonal structure of their corresponding hydroxides, while the Pr_6O_{11} and Er_2O_3 are converted into cubic phase after calcination. TEM was used to examine the morphology and size of the as-prepared RE oxides. As shown in Figure 4, in comparison with that of corresponding RE hydroxides, although the rod-like morphology is briefly maintained, significant changes in length, diameter, and dispersivity are indeed noted. Optimal calcination conditions

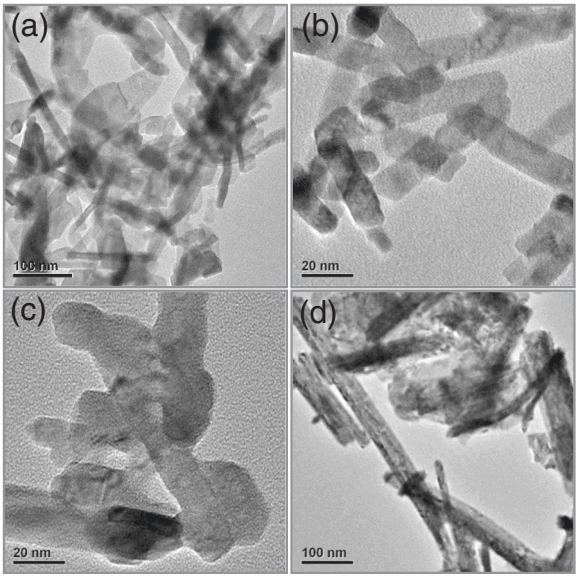

Figure 4 TEM images of La_2O_3 (a), Pr_6O_{11} (b), Nd_2O_3 (c), and Er_2O_3 (d) nanorods. Synthesized by calcinating their corresponding hydroxides at 600°C for 2 h.

to produce RE oxides with well-defined morphology and uniform diameter are yet to be studied in detail.

Conclusions

In summary, we have successfully synthesized the RE (RE = La, Nd, Pr, Sm, Gd, and Er) hydroxide nanorods via a convenient hydrothermal synthetic route. This strategy is called for the first preparation of metal complexes between RE precursors and DDA in water/ethanol mixture at room temperature and subsequent thermal decomposition at elevated temperature. Instead of $Ce(OH)_3$ nanorods, this hydrothermal approach directly resulted in the formation of spherical CeO_2 nanoparticles with very uniform size distributions. By further calcinating the corresponding RE hydroxides at high temperature in air, nanosized RE oxides with remained rod-like morphology could be readily obtained. It is expected that the synthetic route developed in this work could be extended to generate other RE-based nanomaterials.

Additional file

Additional file 1: Supplementary material. Figure S1. FTIR spectra of pure DDA and RE precursor-DDA complexes recovered from the mixture of aqueous RE precursor solution and ethanolic DDA solution. **Table S1.** Textural property of $RE(OH)_3$. **Figure S2.** Histogram of $La(OH)_3$ (a), $Pr(OH)_3$ (b), $Nd(OH)_3$ (c), $Sm(OH)_3$ (d), $Gd(OH)_3$ (e), and $Er(OH)_3$ (f) as synthesized by decomposing the RE precursor-DDA complexes at elevated temperature. The average diameter and related standard derivation are labeled in corresponding figures. **Figure S3.** TEM image (a), HRTEM image (inset of a), and XRD pattern of CeO_2 nanoparticles as prepared by hydrothermal treatment of complexes formed between $CeNO_3$ and DDA. The scale bar for the inset HRTEM image is 2 nm. Figure S4: FTIR spectra of pure DDA and RE precursor-DDA complexes after hydrothermal treatment at elevated temperature.

Competing interest

The authors declare that they have no competing interests.

Authors' contributions

CL and HL performed the materials synthesis and characterization. JY supervised the project and wrote the main manuscript text. All authors read and approved the final manuscript.

Acknowledgements

Financial support from the 100 Talents Program of the Chinese Academy of Sciences and the National Natural Science Foundation of China (Nos.: 21173226 and 21376247) is gratefully acknowledged.

Author details

[1]State Key Laboratory of Multiphase Complex Systems, Institute of Process Engineering, Chinese Academy of Sciences, Beijing 100190, China. [2]University of Chinese Academy of Sciences, No. 19A Yuquan Road, Beijing 100049, China.

Received: 14 January 2015 Accepted: 7 March 2015
Published online: 19 March 2015

References

1. Shen J, Sun L-D, Yan C-H. Luminescent rare earth nanomaterials for bioprobe applications. Dalton Trans. 2008;42:5687–97.
2. Zhou Z, Hu H, Yang H, Yi T, Huang K, Yu M, et al. Up-conversion luminescent switch based on photochromic diarylethene and rare-earth nanophosphors. Chem Commun. 2008;39:4786–8.
3. Si R, Flytzani-Stephanopoulos M. Shape and crystal-plane effects of nanoscale ceria on the activity of Au-CeO_2 catalysts for the water-gas shift reaction. Angew Chem Int Ed. 2008;47:2884–7.
4. Mele P, Artini C, Ubaldini A, Costa GA, Carnasciali MM, Masini R. Synthesis, structure and magnetic properties in the Nd_2O_3–Gd_2O_3 mixed system synthesized at 1200°C. J Phys Chem Solids. 2009;70:276–80.
5. Yamada Y, Segawa M, Sato F, Kojima T, Sato S. Catalytic performance of rare earth oxides in ketonization of acetic acid. J Mol Catal A: Chem. 2011;346:79–86.
6. Gai S, Li C, Yang P, Lin J. Recent progress in rare earth micro/nanocrystals: soft chemical synthesis, luminescent properties, and biomedical applications. Chem Rev. 2014;114:2343–89.
7. Sinclair A, Rodgers JA, Topping CV, Míšek M, Stewart RD, Kockelmann W, et al. Synthesis and properties of lanthanide ruthenium(III) oxide perovskites. Angew Chem Int Ed. 2014;53:8343–7.
8. Zhao Y-L, Song Y-L, Song W-G, Liang W, Jiang X-Y, Tang Z-Y, et al. Progress of nanoscience in China. Front Phys. 2014;9:257–88.
9. Yan Z-G, Yan C-H. Controlled synthesis of rare earth nanostructures. J Mater Chem. 2008;18:5046–59.
10. Wang X, Li Y. Synthesis and characterization of lanthanide hydroxide single-crystal nanowires. Angew Chem Int Ed. 2002;41:4790–3.
11. Song XC, Zheng YF, Wang Y. Selected-control synthesis of dysprosium hydroxide and oxide nanorods by adjusting hydrothermal temperature. Mater Res Bull. 2008;43:1106–11.
12. Xu Z, Li C, Yang P, Zhang C, Huang S, Lin J. Rare earth fluorides nanowires/nanorods derived from hydroxides: hydrothermal synthesis and luminescence properties. Cryst Growth Res. 2009;9:4752–8.
13. Wang P, Bai B, Huang L, Hu S, Zhuang J, Wang X. General synthesis and characterization of a family of layered lanthanide (Pr, Nd, Sm, Eu, and Gd) hydroxide nanowires. Nanoscale. 2011;3:2529–35.
14. Zhang X, Yang P, Wang D, Xu J, Li C, Gai S, et al. $La(OH)_3$:Ln^{3+} and La_2O_3:Ln^{3+} (Ln = Yb/Er, Yb/Tm, Yb/Ho) microrods: synthesis and up-conversion luminescence properties. Cryst Growth Des. 2012;12:306–12.
15. Song Y, You H, Huang Y, Yang M, Zheng Y, Zhang L, et al. Highly uniform and monodisperse Gd_2O_2S:Ln^{3+} (Ln = Eu, Tb) submicrospheres: solvothermal synthesis and luminescence properties. Inorg Chem. 2010;49:11499–504.

16. Yang J, Sargent EH, Kelley SO, Ying JY. A general phase-transfer protocol for metal ions and its application in nanocrystal synthesis. Nat Mater. 2009;8:683–9.
17. Zhang N, Yi R, Zhou L, Gao G, Shi R, Qiu G, et al. Lanthanide hydroxide nanorods and their thermal decomposition to lanthanide oxide nanorods. Mater Chem Phys. 2009;114:160–7.
18. Seitz M, Oliver AG, Raymond KN. The lanthanide contraction revisited. J Am Chem Soc. 2007;129:11153–60.
19. Xin Y, Wang Z, Qi Y, Zhang Z, Zhang S. Synthesis of rare earth (Pr, Nd, Sm, Eu and Gd) hydroxide and oxide nanorods (nanobundles) by a widely applicable precipitation route. J Alloy Compd. 2010;507:105–11.
20. Vekilov PG. What determines the rate of growth of crystals from solution? Cryst Growth Des. 2007;7:2796–810.
21. Vekilov PG. Nucleation. Cryst Growth Des. 2010;10:5007–19.
22. Wang H, Huang W, Han Y. Diffusion–reaction compromise the polymorphs of precipitated calcium carbonate. Particuology. 2013;11:301–8.
23. Neumann A, Walter D. The thermal transformation from lanthanum hydroxide to lanthanum hydroxide oxide. Thermochim Acta. 2006;445:200–4.
24. Ozawa M, Onoe R, Kato H. Formation and decomposition of some rare earth (RE = La, Ce, Pr) hydroxides and oxides by homogeneous precipitation. J Alloy Compd. 2006;408:556–9.